Dynamics of Temperature Profile, Heat and Mass Exchange through Air-Water Interface by Measurements of Thermal Radio Emission Evolution at 60 GHz

Konstantin Gaikovich, Roman V. Troitsky[1]

***Abstract*- On the basis of laboratory measurements of radiobrightness evolution of water at 60 GHz the dynamics of temperature profile (both in the water and in the air) and heat flux through water-air interface have been determined as well as the viscosity sublayer depth in the process of air turbulization.**

I. Introduction

This paper continues radiometry investigations of water thermal regime dynamics [1-2]. The investigation of water near-surface thermal regime by one-wavelength radiobrightness dynamics are especially interesting because temperature gradients in thin subsurface layer and evaporation from water surface determine the heat exchange between ocean and atmosphere.

II. Problem Formulation

Laboratory measurements have been carried out using the equipment which included the water pool with sizes 2 - 1.5 - 0.2 m, radiometer at 60 GHz, two contact temperature pin-transmitters, which could be placed at any depth into water, and a fan placed together with a horn antenna in nadir direction at 1 m above the water surface. The radiometer sensitivity was 0.01 K at integration time $\tau = 1$ s, but taking account of background temperature fluctuations, its real value amounted about 0.03 K. The beam width was 5°, hence the diameter of the beam footprint was about 10 cm. The calibration method used the same water medium at two known values of

[1] Authors are with Radiophysical Research Institute, B.Pecherskaja, 25, Nishny Novgorod, 603600, Russia. E-mail: gai@nirfi.nnov.su. This work was supported by RFBR, grant No.96-02-16514, and by Russian Education Ministry, grant No.95-0-8.1-71.

temperature. The homogeneity and invariability of radiobrightness background as well as its closeness to measured values of brightness temperature (T_B) leads to compensation of surface reflection influence. It made possible to achieve the measurement accuracy comparable with the radiometer sensitivity.

The initial homogeneous temperature distribution in the water was obtained by means of mixing and this distribution was unchanged in the absence of air turbulence during a few minutes interval.The idea consisted of investigation of dynamics appearing after the start of air turbulization. After the fan is switched on, the depth of laminar air layer above the water sharply decreased, and the molecular diffusivity remains the only process in the thin viscosity sublayer above the water surface. Above this layer there exists the air turbulence with the turbulent diffusivity coefficient by some orders more than the molecular one. Because of this reason it was possible to assume that all temperature and humidity changes should take place inside the viscosity sublayer. So, it was possible to use two-layered model for air in turbulent conditions.

The gradients of air parameters are sharply increased along with decreasing of viscosity sublayer depth related with turbulization, which leads to enlargement of vapor flux (evaporation enlargement) from practically zero initial value and, hence, to enlargement of the heat flux related with evaporation. The second component of heat flux related with temperature conductivity also should be changed in this process. As a result one has the fast cooling of water near-surface layer, and this cooling can be measured by high sensitivity radiometer. The following analysis makes possible to retrieve all the details of heat and mass exchange in the air-water system.

The obtained dependence $T_B(t)$ has been used for determination of subsurface temperature profile $T(z,t)$ using the known solution of emission transfer and thermal conductivity equations system [1] for homogeneous half-space $z \leq 0$ with temperature diffusivity coefficient a^2 and radioemission absorption coefficient γ:

$$T(z,t)=\int_{-\infty}^{t} T_B(\tau)(-z)e^{-\frac{z^2}{4a^2(t-\tau)}}\frac{d\tau}{\sqrt{4\pi a^2(t-\tau)^3}}+\frac{1}{\gamma a}\int_{-\infty}^{t} T_B'(\tau)e^{-\frac{z^2}{4a^2(t-\tau)}}\frac{d\tau}{\sqrt{\pi(t-\tau)}},\quad(1)$$

which it is possible to take by parts for region $z < 0$

$$T(z,t)=\int_{-\infty}^{t} T_B(\tau)e^{-\frac{z^2}{4a^2(t-\tau)}}\left[\frac{1}{\gamma}\left(\frac{z^2}{2a^2(t-\tau)}-1\right)-z\right]\frac{d\tau}{\sqrt{4\pi a^2(t-\tau)^3}}\ . \qquad (2)$$

and for z = 0, where (2) is not valid, (1) transformes into

$$T_0(t) = T_B(t) + \frac{1}{\gamma a}\int_{-\infty}^{t} T_B'(\tau)\frac{d\tau}{\sqrt{\pi(t-\tau)}} =$$

$$= T_B(t) + \frac{1}{2\gamma a}\int_{-\infty}^{t} (T_B(t) - T_B(\tau))\frac{d\tau}{\sqrt{\pi(t-\tau)^3}}\ . \qquad (3)$$

The heat flux through water-air interface is determined by time derivative $T'_B(t)$ [1]:

$$J(t) = -\frac{k}{a^2\gamma}\left(T'_B(t) + \gamma a\int_{-\infty}^{t} T'_B(\tau)\frac{d\tau}{\sqrt{\pi(t-\tau)}}\right), \qquad (4)$$

where k is the thermal conductivity coefficient.

For two-layered medium, such as air viscosity sublayer or water thermal film, taking into account the temperature constancy on turbulent-nonturbulent interface $z = -l$ the solution of

thermal conductivity equation gives the subsurface temperature profile as integral of surface temperature:

$$T(z,t)-T(-l)=\frac{2}{l^2}\cdot\int_{-\infty}^{t}T_0(\tau)\sum_{n=1}^{\infty}(-1)^{n+1}\pi n a^2\sin\left(\frac{\pi n(z+l)}{l}\right)\exp\left[\left(\frac{\pi n a}{l}\right)^2(t-\tau)\right]d\tau, \quad (5)$$

and from (5) it follows the expression for brightness temperature dynamics [1]:

$$T_B(t)-T(-l)=\int_{-\infty}^{t}T_0(\tau)\frac{2a^2\gamma}{l^3}\sum_{n=1}^{\infty}(-1)^{n+1}(\pi n)^2\frac{e^{-\gamma l}-(-1)^n}{\left(\frac{\pi n}{l}\right)^2+\gamma^2}\exp\left(\left(\frac{\pi n a}{l}\right)^2(t-\tau)\right)d\tau. \quad (6)$$

Unlike the case of homogeneous medium the inversion formula for this equation is unknown but it is possible to solve (6) numerically as Volterra's equation of the 1-st kind with variable upper limit relative $T_0(t)$, and then, substituting it into (5), to determine the temperature profile $T(z,t)$ and heat flux $J(t) = -k\frac{\partial T}{\partial z}(0,t)$.

In the frameworks of above mentioned model the heat flux $J(t)$ is the sum of the first component related with evaporation, and the second one related with molecular temperature conductivity in viscosity sublayer:

$$J(t) = J_q(t) + J_T(t) = -r\rho D_q\frac{dq}{dz}(0) - k\frac{dT}{dz}(0) = -r\rho D_q\frac{q_a - q(0)}{d} - \rho c_p a^2\frac{T_a - T(0)}{d}, \quad (7)$$

where q is water vapor concentration, r is specific heat of evaporation, ρ is air density, D_q is vapor diffusivity coefficient, c_p is specific heat capacity at the constant pressure, d is the viscosity sublayer depth, q_a, T_a are values of vapor concentration and temperature respectively on the

turbulent-nonturbulent interface. The air density $\rho = \frac{1}{R_a}\frac{P}{T}$, where P is air pressure and R_a is gaseous constant of air.

It was obtained that the typical relaxation time to linear profiles of temperature and vapor concentration in the viscosity sublayer is about 0.2 s, hence it is possible to suppose that the temperature and concentration gradients are constants. The water vapor concentration at the water surface $q(0)$ can be expressed through saturated concentration:

$$q(0) = q_s(1 - \frac{J_q}{J_0}), \tag{8}$$

where J_0 is the maximum heat flux which can be achieved by evaporation in vacuum:

$$J_0 = \frac{r\rho_w}{\eta}\sqrt{\frac{KT(0)}{2\pi m}}\, e^{-\frac{mr}{KT(0)}}, \tag{9}$$

where η is near-unity constant, K is the Boltzmann's constant, m is the water molecula mass, ρ_w is water density. One can see that all the parameters in (9) depend only on water surface temperature, hence it is possible to determine the viscosity sublayer depth d by values of J and T_0, which can be obtained by measured radiobrightness evolution. It makes possible to distinguish two components of heat flow. The substitution (8) into (7) gives

$$J = b_1\frac{q_s - q_a}{d + \frac{b_1 q_s}{J_0}} - b_2\frac{T_a - T(0)}{d}, \tag{10}$$

where $b_1 = r\rho D_q$, $b_2 = \rho c_p a^2$ depend only on $T(0)$. It is easy to obtain from (10) the quadratic equation relative the viscosity sublayer depth d:

$$d^2 J + d[J \frac{b_1 q_s}{J_0} - b_1(q_s - q_a) + b_2(T_a - T(0))] + b_1 b_2 \frac{q_s}{J_0}(T_a - T(0)) = 0 \qquad (11)$$

In general, both solutions have the physical meaning. The second solution of (11) (with minus at square root) can be achieved at more high level of turbulence and only if air is warmer than water and two heat flux components have the opposite directions.

III. Investigations of Temperature and Heat Flux Dynamics

The brightness temperature dynamics in the process of air turbulization has been observed. At time $t = 0$ the fan is switched on and the fast cooling of water near-surface layer begins. After the time $t = 100$ s the contact temperature measurements give the periodic temperature variations related with the convection process in unstable stratified water layer. The Rayleigh number which determines the possibility of convection process achieves its critical value $R = 1708$ at this time, so the necessary condition of convection is satisfied afterwards (for t > 100 s). It is clear that the retrieval results under convection would be not true, so the duration of turbulization should be less then 100 s.

In the Fig.1 an example of measurements for two sequential turbulization cycles is given. In the first cycle the fan was switched off at time of convection beginning $t = 100$ s and in the second cycle - at $t = 60$ s (before the convection appearing). The observed dynamics of heat flux components allows the simple physical interpretation. After the evaporation achieves its maximum it begins to decrease because of decreasing of vapor saturation concentration, which is caused by water surface cooling. It is possible also to obtain the evaporation rate $I_q (t) = \frac{1}{r} J_q(t)$. Its maximum value was about 0.05 g/m^{2}s . In the Fig.2 it is possible to see the corresponding

retrieved and contact measured temperature evolution at the depth $z = -0.2$ cm. The difference between retrieved and contact temperatures in end of the first cicle is related with convection beginning. In the second cicle (without the convection) the retrieval is irreproachable. The mean square difference between retrieved and contact temperatures is 0.07 K. In this case the air was warmer then the water by 3 K.

The viscosity sublayer depth in the air determined from (12) amounts about 0.2 cm. If we have the retrieved surface temperature as a boundary condition, it is possible to determine the temperature profile evolution in the air viscosity sublayer from the solution (5) for two-layered medium. In the Fig.3 the retrieved temperature dynamics in two sequential air turbulization cyrcles on both sides of air-water interface is shown.

It was very interesting to investigate the case of turbulent water because in real conditions such a situation is typical. It is well known that in the near-surface water layer with the depth of some millimeters the turbulence is absent and the heat transfer is determined by molecular diffusivity, so the temperature gradients in these laminar layers called "thermal films" are respectively by some orders more than in turbulent water, and it is possible to consider the temperature below the lower boundary of thermal film as constant. The temperature overfalls in the thermal films are typically of about 1 K.

The radiobrightness dynamics for cases of turbulent and nonturbulent water in the air turbulization cyrcle is given in the Fig.4. The water turbulence was made by rapid mixing at the pool bottom. The dynamics in both cases was almost the same up to time $t = 10$ s when in the turbulent case the cooling achieves the lower boundary of the thermal film. After this time, the cooling in the nonturbulent case moves into more deep water layers, but in the turbulent case the temperature at the lower boundary of the thermal film must be constant (the same as in turbulent region). The analysis of the case of turbulent water has been carried out on the basis of the expressions (5-6) for two-layered medium where the depth of the thermal film d_T as a free

parameter has been used. It is possible to obtain the depth of the thermal film using the fact that in both turbulent and nonturbulent cases the air viscosity sublayer depth must be the same. The analysis of heat fluxes gives the value d_T =0.18 cm. The simple method to estimate the thermal film depth can be based on the time of beginning of radiobrighness divergence from nonturbulent case. The time t_d of temperature disturbance diffusion from the surface to the depth z is (at 99% level for unity surface temperature overfall $t_d = 3.5\, t^*$ where $t^* = z^2/a^2$ [1]) t_d = 10 s. From this we have about the same value $z = d_T = 0.20$ cm.

In the thermal films there is no convection. Because the retrieved temperature profile in the thermal film was almost everywhere close to linear, it was easy to determine the Rayleigh number, which was always less than 80 , i.e. very far from its critical value.

IV. Conclusion

These methods can be applied in the real conditions because for measurements at the frequency 60 GHz the reflection influence would be also well compensated.

References

[1]. K.P.Gaikovich, "Simultaneous solution of emission transfer and thermal conductivity equations in the problems of atmosphere and subsurface radiothermometry," *IEEE Trans.Geosci.Remote Sens.*, vol.32, pp.885-889, 1994.

[2]. K.P.Gaikovich, A.N.Reznik and R.V.Troitskii, "Microwave subsurface profile thermometry," *Dig.IGARSS'91*, Univ. Technol., Espoo, Finland, vol.3, pp.1195-1198, 1991.

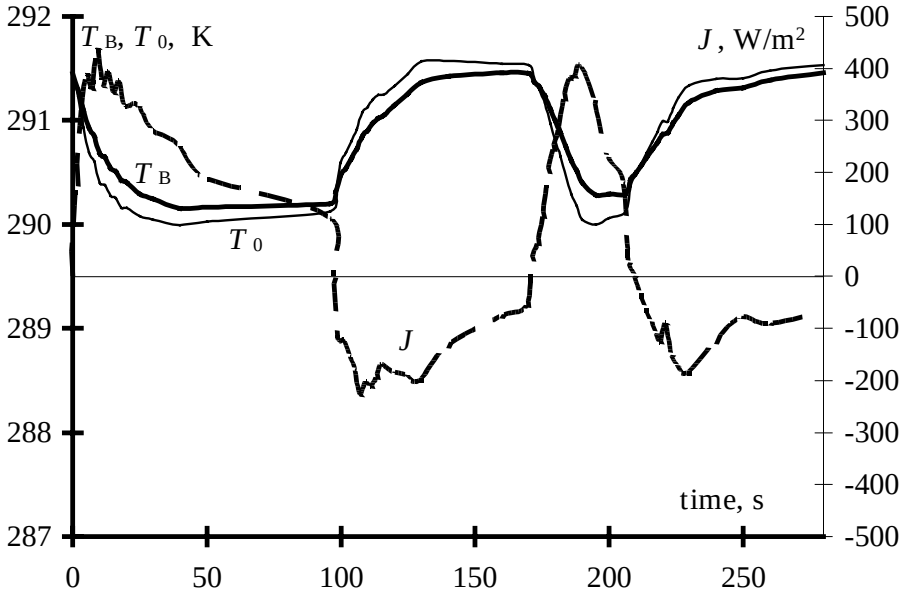

Fig.1. Brightness temperature dynamics (T_B) and retrieved heat flux (J) and surface temperature (T_0) in two sequential cycles.

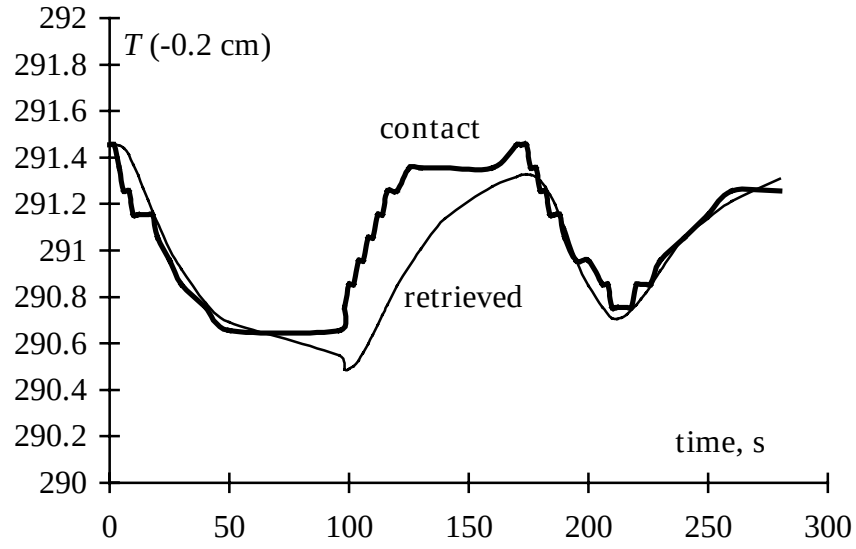

Fig.2. Retrieved and contact measured temperature evolution at the depth $z = -0.2$ cm for the case shown in Fig.1.

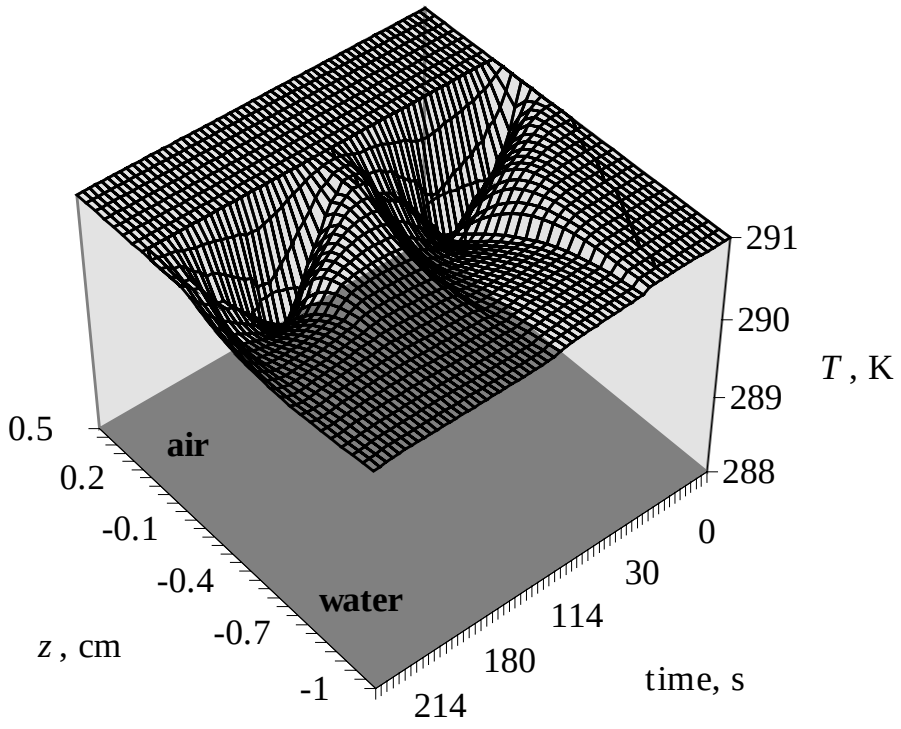

Fig.3. Temperature retrieval in two sequential air turbulization cyrcles on both sides of air-water interface for the case shown in Fig.1.

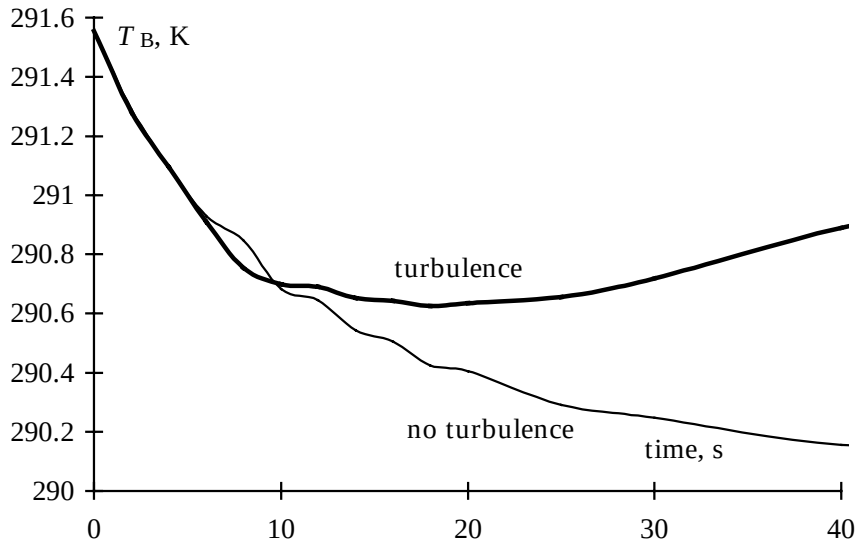

Fig.4. The radiobrightness dynamics for turbulent and nonturbulent water.

Figure captures:

Fig.1. Brightness temperature dynamics (T_B) and retrieved heat flux (J) and surface temperature (T_0) in two sequential cycles.

Fig.2. Retrieved and contact measured temperature evolution at the depth z = –0.2 cm for the case shown in Fig.1.

Fig.3. Temperature retrieval in two sequential air turbulization cyrcles on both sides of air-water interface for the case shown in Fig.1.

Fig.4. The radiobrightness dynamics for turbulent and nonturbulent water.